

Stabilization of quantum information by combined dynamical decoupling and detected-jump error correction

D. Geberth¹, O. Kern^{1,a}, G. Alber¹, and I. Jex²

¹ Institut für Angewandte Physik, Technische Universität Darmstadt, 64289 Darmstadt, Germany

² Department of Physics, FJFI ČVUT, Břehová 7, 115 19 Praha 1 - Staré Město, Czech Republic

Received 9 July 2007 / Received in final form 5 October 2007

Published online 31 October 2007 – © EDP Sciences, Società Italiana di Fisica, Springer-Verlag 2007

Abstract. Two possible applications of random decoupling are discussed. Whereas so far decoupling methods have been considered merely for quantum memories, here it is demonstrated that random decoupling is also a convenient tool for stabilizing quantum algorithms. Furthermore, a decoupling scheme is presented which involves a random decoupling method compatible with detected-jump error correcting quantum codes. With this combined error correcting strategy it is possible to stabilize quantum information against both spontaneous decay and static imperfections of a qubit-based quantum information processor in an efficient way.

PACS. 03.67.Pp Quantum error correction and other methods for protection against decoherence – 03.67.Lx Quantum computation

1 Introduction

Quantum information processing of many-qubit systems requires efficient methods for protecting arbitrary logical quantum states against unwanted environmental interactions or uncontrolled inter-qubit couplings. So far, two strategies have been developed for achieving this goal, namely dynamical decoupling and redundancy-based quantum error correction. Dynamical decoupling [1] is based on the main idea of suppressing unwanted influences on the quantum dynamics by appropriately applied deterministic or stochastic external forces. A disadvantage of this approach is that typically residual errors are left. An advantage of this method of error suppression is that the complete physically available Hilbert space can be used for logical information processing. In redundancy-based error correction (see [2], Chap. 10) only a subspace of the physically available Hilbert space can be used for logical information processing. This subspace has to be selected in such a way that possible errors can be corrected perfectly by appropriate control measurements and recovery operations. Thus, this latter type of error correction typically requires a sufficiently large number of redundant qubits which cannot be used for logical purposes. This represents a serious disadvantage if only quantum information processors with small numbers of qubits are available. Thus, in view of nowadays technology it is desirable to develop error correcting strategies which combine the positive advantages of both approaches in order to achieve the high-

est possible degree of error suppression with the smallest possible number of redundant qubits. Combined methods in which environmental interactions are corrected by redundancy-based quantum error correction and in which uncontrolled inter-qubit couplings within a quantum information processor are suppressed by dynamical decoupling may offer interesting perspectives for the stabilization of few-qubit quantum information processors against unwanted errors.

In the following such a combined error correction scheme is presented. The main problem which has to be overcome in this context is compatibility. One has to ensure that the chosen dynamical decoupling method does not leave the code space of the redundancy-based quantum error correction method. If this compatibility cannot be guaranteed uncorrectable errors may arise. Furthermore, in practical applications one is also interested in minimizing the residual errors originating from errors during recovery operations, for example, and from the dynamical decoupling method itself. Currently, no universal solution is available for this compatibility and optimization problem.

Here, first results and solutions of these compatibility and optimization problems are presented for a particular combined error correcting method which is capable of correcting a special case of environmentally-induced decoherence, namely spontaneous decay of qubits. Such decay processes may arise from spontaneous emission of photons, for example. In our subsequent discussion we concentrate on the special but important case that spontaneous

^a e-mail: oliver.kern@physik.tu-darmstadt.de

decay processes affecting different qubits are statistically independent. This implies that in principle not only error times but also error positions can be determined by observation of the individual qubits. In the context of photon-induced spontaneous decay this case is realized whenever the wave lengths of spontaneously emitted photons are significantly smaller than the spatial separations between adjacent qubits. Under these circumstances detected-jump error correcting quantum codes [3,4] can be used for an efficient redundancy-based correction of resulting errors. As an additional source of errors we consider uncontrolled inter-qubit couplings within a quantum information processor which can be modeled by Heisenberg-type couplings with unknown parameters. It has been demonstrated recently that such errors can be suppressed significantly with the help of embedded dynamical decoupling methods in which a deterministic dynamical decoupling scheme is embedded into a stochastic one [5]. The deterministic decoupling scheme leads to a significant error suppression for short times whereas the stochastic decoupling method guarantees that the residual error-induced exponential decay of the fidelity of any quantum state is linear-in-time only and not quadratic as in the case of a pure deterministic scheme [6,7].

This paper is organized as follows. In Section 2 basic concepts of deterministic, stochastic, and embedded dynamical decoupling methods are summarized briefly. In Section 3 the error suppressing potential of stochastic dynamical decoupling methods is studied quantitatively with the help of the entanglement fidelity. This latter quantity is identical to the mean fidelity for large numbers of qubits. Whereas previously derived rigorous lower bounds [6] tend to overestimate the fidelity decay of a quantum memory significantly this mean fidelity yields reliable quantitative estimates on the mean accuracy of achievable stabilization properties for both quantum memories and quantum computations. In Section 4, finally, a new combined error correcting scheme is introduced in which a compatible embedded dynamical decoupling scheme is applied within a detected-jump correcting quantum code space. This way static random imperfections and spontaneous decay processes can be suppressed simultaneously.

2 Dynamical decoupling – Basic concepts

Let us consider a quantum system S whose Hilbert space \mathcal{H}_S is of dimension N . Typically S represents a quantum register containing n_q qubits so that $N = \dim \mathcal{H}_S = 2^{n_q}$. The time evolution $U(t)$ of S is due to a time dependent Hamiltonian $H(t) = H_0 + H_c(t)$ which is the sum of a static term we would like to suppress (this term may represent imperfections in a quantum computer, for example), and a time dependent term which represents the control operations we are able to apply. Dynamical decoupling tries to achieve a suppression of H_0 .

According to the Schrödinger equation our system evolves in time as

$$U(t) = \mathcal{T} \exp \left(-i \int_0^t H(\tau) d\tau / \hbar \right). \quad (1)$$

Analogous to (1) let us denote the time evolution due to $H_c(t)$ alone by $U_c(t)$, i.e.,

$$U_c(t) = \mathcal{T} \exp \left(-i \int_0^t H_c(\tau) d\tau / \hbar \right). \quad (2)$$

(\mathcal{T} denotes the time ordering operator.) The time evolution in the so called toggled frame $\tilde{U}(t) = U_c^\dagger(t)U(t)$ is determined by the Schrödinger equation

$$i\hbar \frac{d\tilde{U}(t)}{dt} = \tilde{H}(t)\tilde{U}(t), \quad \tilde{H}(t) = U_c^\dagger(t)H_0U_c(t). \quad (3)$$

In a simplified scenario the time dependence of $H_c(t)$ involves sequences of δ -pulses applied at times $t_i = i\Delta t$, $i \in \mathbb{N}$. This time evolution gives rise to so-called unitary bang-bang pulses of the form $g_{f(i)}g_{f(i-1)}^\dagger$, whereas the i th pulse is the product of elements g which are chosen from a set of unitary operators \mathcal{G} according to a certain selection rule $f(i)$. For the corresponding time evolution due to $H_c(t)$ we obtain

$$U_c(t) = g_{f(i)}, \quad (i-1)\Delta t \leq t \leq i\Delta t \quad (4)$$

and the Hamiltonian $\tilde{H}(t)$ of the toggled frame becomes piecewise constant, i.e.,

$$\tilde{H}(t) = g_{f(i)}^\dagger H_0 g_{f(i)}, \quad (i-1)\Delta t \leq t \leq i\Delta t. \quad (5)$$

In the following several selection rules $f(i)$ and their advantages and disadvantages will be discussed. They give rise to periodic (or cyclic) decoupling, random decoupling, and embedded decoupling schemes.

2.1 Periodic decoupling

Let us choose $f(i) = (i-1 \bmod n_c) + 1$ so that $U_c(t)$ reduces to a set of n_c periodically repeating unitary transformations $g_{f(i)} \in \mathcal{G}$ (compare with Fig. 1a). This leads to a cyclic unitary control transformation, i.e.,

$$U_c(t + T_c) = U_c(t), \quad T_c = n_c \Delta t. \quad (6)$$

We can use average Hamiltonian theory (AHT) [8] to express the unitary time evolution operator of the toggled frame at integer numbers n of cycles as

$$\tilde{U}(nT_c) = \exp \left(-i \overline{H} n T_c / \hbar \right). \quad (7)$$

Thereby, \overline{H} is given by the Magnus expansion $\overline{H} = \overline{H}^{(0)} + \overline{H}^{(1)} + \overline{H}^{(2)} + \dots$ [8]. In the limit of fast control sequences, i.e. $T_c \rightarrow 0$ and $M \rightarrow \infty$ for a given time $T = MT_c > 0$, it is sufficiently accurate to consider lowest order AHT yielding

$$\overline{H}^{(0)} = \frac{1}{T_c} \int_0^{T_c} dt_1 \tilde{H}(t_1) = \frac{1}{n_c \Delta t} \sum_{i=1}^{n_c} g_i^\dagger H_0 g_i \Delta t. \quad (8)$$

In order to achieve the main goal of dynamical decoupling, namely a vanishingly small total time evolution in the

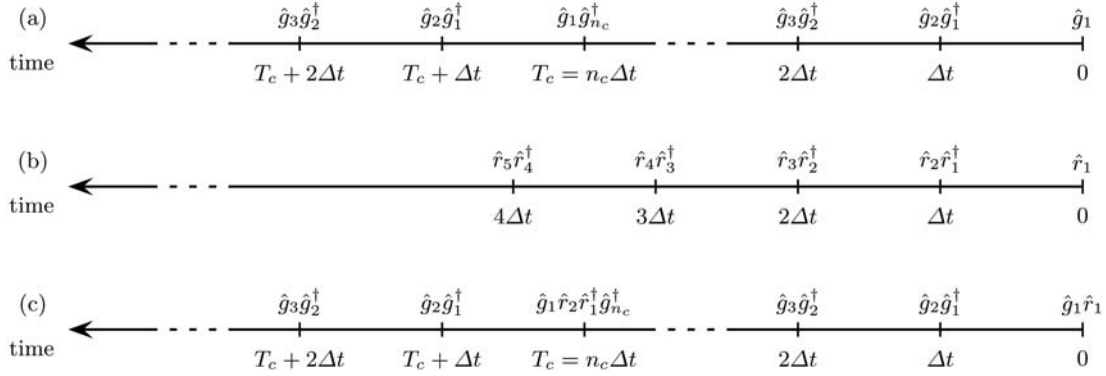


Fig. 1. Schematic representation of: (a) periodic dynamical decoupling (PDD) $g \in \mathcal{G}$, (b) naive random decoupling (NRD) $r \in \mathcal{G}$, (c) embedded decoupling (EMD) $g \in \mathcal{G}$ and $r \in \mathcal{G}'$. The time evolution between subsequent instantaneously applied unitary operations is assumed to be governed by a perturbing Hamiltonian \hat{H}_0 .

toggled frame, $\overline{H}^{(0)}$ has to vanish. This latter requirement can be fulfilled by selecting a set \mathcal{G} of unitary operations, for example, for which the relation

$$\sum_{g \in \mathcal{G}} g^\dagger H_0 g = 0 \tag{9}$$

holds. Such a set \mathcal{G} of size $n_c = |\mathcal{G}|$ we call a decoupling set¹ for the Hamiltonian H_0 . This first order decoupling works perfectly only in the limit of fast control sequences.

Viola and Knill [6] calculated a lower bound for the worst case fidelity

$$F_w(T = nT_c) = \min_{|\psi\rangle} |\langle \psi | \tilde{U}(T) | \psi \rangle|^2 \tag{10}$$

which is valid for arbitrary periodic dynamical decoupling (PDD²) sequences. In particular, they showed

$$F_w^{\text{PDD}} > 1 - \mathcal{O}(T^2 T_c^2 \kappa^4) \tag{11}$$

with $\kappa = \|H_0\|_2$ denoting the operator-2 norm of the internal Hamiltonian H_0 .

A common procedure for obtaining higher than lowest order decoupling is to engineer each cycle in such a way that is it time symmetric. This can be achieved by traversing an original cycle \mathcal{G} after its completion again backwards so that the relation $\tilde{H}(T'_c - t) = \tilde{H}(t)$ holds with $T'_c = 2T_c$. In such a case all terms of odd orders in the Magnus expansion vanish and one obtains the improved bound [10]

$$F_w^{\text{SDD}} > 1 - \mathcal{O}(T^2 T_c^4 \kappa^6). \tag{12}$$

Thereby, SDD stands for symmetric dynamic decoupling.

A disadvantage of periodic (or cyclic) decoupling is the quadratic time dependence of the fidelity decay and its dependence on the length of the sequence. As a consequence for long times and/or large decoupling sets \mathcal{G} the accumulating errors might increase quickly.

¹ On how to construct such a set see e.g. [9].

² The abbreviations for the different decoupling methods are adopted from [10].

2.2 Annihilators

We defined a decoupling set \mathcal{G} for a Hamiltonian H_0 as a set of unitary operation $g \in \mathcal{G}$ such that

$$\sum_{g \in \mathcal{G}} g^\dagger H_0 g = 0. \tag{13}$$

We will call a decoupling set for which the above equation holds for all traceless Hamiltonians an annihilator. It was shown in [11] that such a set contains at least N^2 elements. An annihilator can always be chosen to be also a so-called nice error basis, which is a unitary and orthonormal operator basis fulfilling some additional convenient properties (for a detailed definition see [12]). Since the elements of a nice error basis form an irreducible projective representation of an underlying index group Schur's lemma implies the important relation [11]

$$\frac{1}{|\mathcal{G}|} \sum_{g \in \mathcal{G}} g^\dagger H_0 g = \frac{\text{tr } H_0}{N} \mathcal{I}. \tag{14}$$

In our subsequent discussion we will take as annihilator the nice error basis

$$\mathcal{P} = \{\mathcal{I}, X, Y, Z\}^{\otimes n_q}, \tag{15}$$

which consists of tensor products of the Pauli matrices,

$$\mathcal{I} = \begin{pmatrix} 1 & 0 \\ 0 & 1 \end{pmatrix}, X = \begin{pmatrix} 0 & 1 \\ 1 & 0 \end{pmatrix}, Y = \begin{pmatrix} 0 & -i \\ i & 0 \end{pmatrix}, Z = \begin{pmatrix} 1 & 0 \\ 0 & -1 \end{pmatrix}. \tag{16}$$

However, any other annihilator would lead to the same results.

2.3 Random decoupling

Let us choose $f(i) \in_R \{1, 2, \dots, n_c\}$, i.e. elements $f(i)$ are selected randomly from the set $\{1, 2, \dots, n_c\}$ giving rise to randomly selected unitary transformations $r_i = g_{f(i)}$ (see Fig. 1b). To calculate the worst case mean

fidelity of such a naive random decoupling (NRD) scheme we consider the average over all realizations of the r_i which we will denote by \mathbf{E} , i.e.,

$$F_w(T = n\Delta t) = \min_{|\psi\rangle} \mathbf{E} |\langle \psi | \mathcal{I}^\dagger \tilde{U}(T) | \psi \rangle|^2. \quad (17)$$

For the moment we call this decoupling scheme ‘naive’ since there are more sophisticated decoupling methods which will be discussed in the next section. It was shown in [6] that this mean fidelity obeys the inequality

$$F_w^{\text{NRD}} > 1 - \mathcal{O}(T\Delta t\kappa^2). \quad (18)$$

An advantage of NRD methods versus periodic methods is the linear time dependence of the fidelity decay and its independence of the length of the decoupling set \mathcal{G} . However, at the same time the error suppression is weaker (compare the factor κ^2 of (18) with the factors κ^4 of (11) or κ^6 of (12)). As a consequence of this independence it is always possible to draw the random unitary transformations from an annihilator, such as $\mathcal{G} = \mathcal{P}$. However, choosing a particularly adjusted decoupler \mathcal{G} for a Hamiltonian H_0 may offer advantages if one is restricted to particular unitary transformations.

In addition NRD schemes are well suited for stabilizing quantum algorithms against perturbations [7]. This aspect will be discussed in detail in Section 3. In the latter reference we introduced the term Pauli-random-error-correction (PAREC) for the stabilization of a quantum computation using NRD decoupling with $\mathcal{G} = \mathcal{P}$.

2.4 Embedded decoupling

In embedded decoupling (EMD) schemes two different sets of decoupling operations are used, namely a set \mathcal{G} which achieves (at least) first order decoupling for a perturbing Hamiltonian H_0 and an annihilator \mathcal{G}' .

Using decoupling operations in a deterministic way from a set \mathcal{G} for PDD [or SDD] we obtain an effective time evolution which can be described by $\exp(-i\overline{H}T_c)$. According to (9) the Magnus expansion yields $\overline{H}^{(0)} = 0$ for a PDD scheme [and $\overline{H}^{(0)} = \overline{H}^{(1)} = 0$ for a SDD scheme]. We can suppress \overline{H} even further by applying a NRD scheme involving a set of unitary operations \mathcal{G}' . Thereby, random unitary operations from this set are applied inbetween any two PDD or SDD cycles (compare with Fig. 1c).

A bound on the worst case fidelity we can obtain by simply taking the NRD bound of (18) and replacing Δt by T_c and κ by a bound on the norm of \overline{H} . Thus one finds the results [5]

$$F_w^{\text{EMD}} > 1 - \mathcal{O}(TT_c^3\kappa^4) \quad (19)$$

for an embedded decoupling scheme (EMD) based on an underlying PDD scheme and [10]

$$F_w^{\text{SEMD}} > 1 - \mathcal{O}(TT_c^5\kappa^6) \quad (20)$$

for a symmetric embedded decoupling scheme (SEMD) based on an underlying SDD scheme.

Alternatively one may achieve comparably good results by using random path decoupling schemes as discussed in [10]. In these schemes one uses a PDD (or SDD) scheme based on a set \mathcal{G} and in each cycle j the selection rule $f_j(i) = \pi_j((i - 1 \bmod n_c) + 1)$ is used. Thereby, π_j is a permutation of the set $\{1, 2, \dots, n_c\}$ chosen at random and independently for each cycle.

3 Stabilizing quantum algorithms against static imperfections by naive random decoupling

As mentioned in Section 2.3 naive random decoupling (NRD) can be used to stabilize arbitrary quantum algorithms against static imperfections in a rather simple way. In this section basic properties of this stabilization are explored quantitatively. As a quantitative measure for the accuracy of stabilization the expectation value of the entanglement fidelity is used which is approximately equal to the average fidelity in the case of high dimensional quantum systems. Numerical results demonstrating characteristic stabilization properties of the recently proposed PAREC method are presented for the special case of the quantum Fourier transform. In particular, they are compared with the recently proposed stabilization method of Prosen et al. [13].

3.1 Entanglement fidelity and average fidelity

The bound (18) was calculated for the worst case fidelity. Typically this bound overestimate the actual fidelity decay to a high degree. Therefore, for practical purposes it is more convenient to consider other fidelity measures, such as the average fidelity

$$\overline{F}(\mathcal{E}) = \int d\psi \langle \psi | \mathcal{E}(|\psi\rangle\langle\psi|) | \psi \rangle \quad (21)$$

or the entanglement fidelity

$$F_e(\mathcal{E}) = \langle \phi | (\mathcal{I} \otimes \mathcal{E})(|\phi\rangle\langle\phi|) | \phi \rangle. \quad (22)$$

Thereby, the integration involved in the definition of the average fidelity (21) has to be performed over the uniform (Haar) measure on the relevant quantum state space with the normalization $\int d\psi = 1$ and \mathcal{E} denotes a trace-preserving quantum operation, i.e. a general completely positive map. The pure quantum state $|\phi\rangle$ occurring in the definition of the entanglement fidelity is a maximally entangled state between the quantum system under consideration and an ancilla system of the same dimension N . Furthermore, \mathcal{I} denotes the identity operation acting on the ancilla system. Accordingly, the entanglement fidelity measures the degree to which the entanglement of quantum state is preserved by a quantum operation \mathcal{E} . Apparently, it is independent of the choice of the maximally entangled state since any two maximally entangled states are related by a unitary acting only on the ancilla.

Both fidelity measures are not independent but are related by [14,15]

$$\overline{F}(\mathcal{E}) = \frac{NF_e(\mathcal{E}) + 1}{N + 1} = F_e(\mathcal{E}) + \mathcal{O}\left(\frac{1 - F_e(\mathcal{E})}{N}\right). \quad (23)$$

Thus, in the case of high dimensional quantum systems, i.e. $N = 2^{n_q} \gg 1$, the difference between both measures tends to zero.

In the following we are mainly interested in the entanglement fidelity comparing a unitary operation U and its slightly perturbed version U_δ . Thus the relevant quantum operation \mathcal{E} involves a single unitary Kraus operator K which is given by $K = U^\dagger \cdot U_\delta$. On the basis of (23) in the case of high dimensional quantum systems the average fidelity is approximately given by the entanglement fidelity

$$F_e(U^\dagger \circ U_\delta) = \left| \frac{1}{N} \text{tr}\{U^\dagger U_\delta\} \right|^2 \quad (24)$$

which is determined by the absolute square of a fidelity amplitude

$$A = \frac{1}{N} \text{tr}\{U^\dagger U_\delta\}. \quad (25)$$

Typically, the evaluation of this fidelity amplitude is much simpler than the direct evaluation of the average fidelity (21). Therefore, in view of its close relationship to the average fidelity our subsequent discussion will concentrate on the behavior of the entanglement fidelity mainly.

3.2 Static imperfections and short-time behavior of the fidelity

Typically, the fundamental unitary transformation U constituting a quantum algorithm can be decomposed into a sequence of n_g elementary one- and two-qubit quantum gates, i.e.,

$$U = U_{n_g} \dots U_3 U_2 U_1. \quad (26)$$

Let us assume in our subsequent discussion that the quantum algorithm under consideration involves t interactions of such a fundamental unitary transformation U . Such quantum algorithms appear in the context of search algorithms, for example [16]. Furthermore, let us focus our attention on the case of static imperfection in which the perturbing influence on such a quantum algorithms arises from unknown (but fixed and time independent) Hamiltonian coupling H_0 between the qubits constituting the quantum information processor. In the idealized situation that the controlled elementary quantum gates U_j , $j = 1, \dots, n_g$ are performed instantaneously after time intervals of duration Δt during which unknown inter-qubit couplings perturb the quantum algorithms in the τ th interaction the ideal quantum gate U_j is replaced by the perturbed unitary quantum gate

$$U_j \mapsto U_\delta(\tau) = \exp(-i\delta H_j^\tau) U_j \quad (27)$$

with $\delta H_j^\tau = H_0 \Delta t / \hbar$. In the notation of (27) the index $\tau = 1, \dots, t$ takes into account that the perturbations

could be different for successive iterations of the algorithm. However, in the case of static imperfections considered here this possible complication is not relevant. In Appendix A it is shown that after t iterations and for sufficiently short times $T = tn_g \Delta t$ according to second order time-dependent perturbation theory the fidelity amplitude A is given by

$$\begin{aligned} F_e(t) &= |A(t)|^2 \\ &= 1 - 2 \sum_{j,k=1}^{n_g} \frac{1}{N} \text{tr}\{U_{1\dots j}^\dagger \delta H U_{j\dots 1} U_{1\dots k}^\dagger \delta H U_{k\dots 1}\} \\ &\quad - 2 \sum_{\tau=1}^{t-1} (t - \tau) \sum_{j,k=1}^{n_g} \frac{1}{N} \text{tr}\{U^{-\tau} U_{1\dots j}^\dagger \delta H U_{j\dots 1} \\ &\quad \times U^\tau U_{1\dots k}^\dagger \delta H U_{k\dots 1}\} + \mathcal{O}(\delta H^3). \end{aligned} \quad (28)$$

Thereby, the first term in the sum of (28) describes the influence of perturbations occurring in the same iteration τ and the second double sum describes their influence in different iterations. This particular form of the short-time behavior of the fidelity amplitude has been studied in detail by Frahm et al. [17]. In particular, these authors demonstrated that whenever an ideal unitary transformation of a quantum map U can be modeled by a random matrix for sufficiently short times after t iterations the corresponding decay of the entanglement fidelity is given

$$F_e(t) \approx 1 - \frac{t}{t_c} - \frac{2}{\sigma} \frac{t^2}{t_c N} \quad (29)$$

where $1/t_c \approx n_g^2 \text{tr}\{H_0^2\} \Delta t^2 / N$ and σ denotes the relative fraction of the chaotic component of the phase space of this map. Furthermore, numerical studies indicate that the behavior of higher order terms is such that the fidelity decay becomes approximately exponential, i.e.,

$$F_e(t) \approx \exp\left(-\frac{t}{t_c} - \frac{2}{\sigma} \frac{t^2}{t_c N}\right). \quad (30)$$

3.3 Suppression of static imperfections by increasing the decay of correlations

In special cases in which an ideal unitary transformation U is not decomposed into elementary gates we may simplify (28) by taking $n_g = 1$ thus obtaining the short-time fidelity decay

$$F_e(t) = 1 - \sum_{\tau=-(t-1)}^{t-1} (t - |\tau|) \frac{1}{N} \text{tr}\{U^{-\tau} \delta H U^\tau \delta H\} + \mathcal{O}(\delta H^3). \quad (31)$$

This expression has been studied previously by Prosen [13]. It indicates that the faster the decay of the correlation function

$$\frac{1}{N} \text{tr}\{U^{-\tau} \delta H U^\tau \delta H\}$$

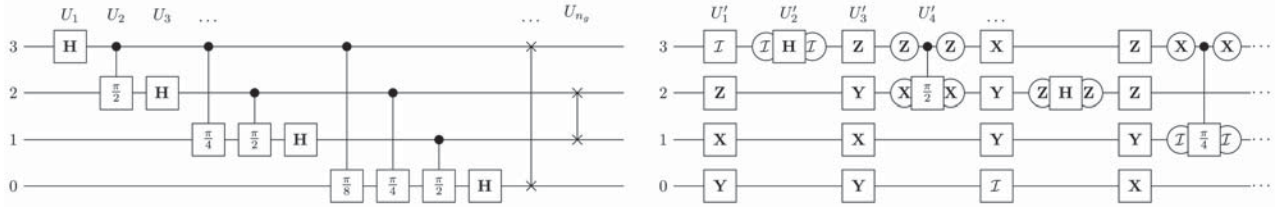


Fig. 2. Quantum circuit of the Quantum-Fourier-Transformation for $n_q = 4$ qubits (left panel). The first four gates of the same circuit involving the PAREC method (right panel).

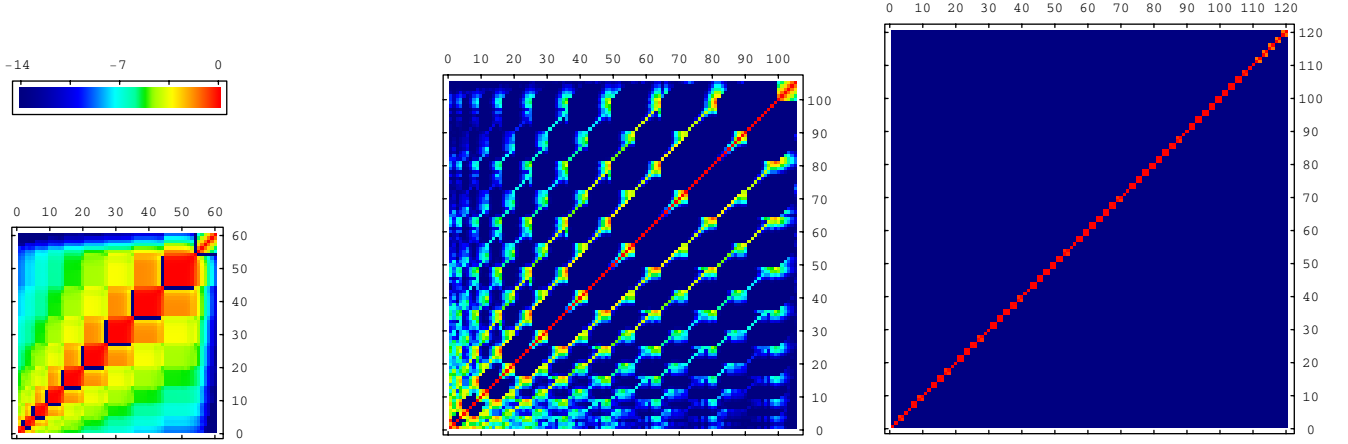


Fig. 3. (Color online) $\ln [(\langle C(j, k) \rangle + 1/N^2)/\delta^2]$ for the QFT with $n_q = 10$ qubits using the usual gate decomposition with $n_g = 60$ gates (left panel), the decomposition by Prosen using $n'_g = 105$ gates (middle panel) and $\ln [(\mathbf{E}\langle C(j, k) \rangle + 1/N^2)/\delta^2]$ using the PAREC method with $n'_g = 2n_g = 120$ gates (right panel).

the slower the decay of the fidelity. According to an original proposal by Prosen and Žnidarič [18] this characteristic feature of the fidelity decay can be exploited for stabilizing a quantum algorithm against static imperfections. This aspect was investigated in detail by these authors for the special case of $t = 1$. In this case (28) reduces to the simpler form

$$F_e = 1 - \sum_{j,k=1}^{n_g} \frac{1}{N} \text{tr}\{U_{1\dots j}^\dagger \delta H U_{j\dots 1} U_{1\dots k}^\dagger \delta H U_{k\dots 1}\} + \mathcal{O}(\delta H^3) \\ \equiv 1 - \sum_{j,k=1}^{n_g} C(j, k) + \mathcal{O}(\delta H^3). \quad (32)$$

Prosen and Žnidarič based their error suppression method on the idea to rewrite a quantum algorithm U in such a way that for the new gate decomposition the sum over the off-diagonal elements of the correlation matrix $C(j, k)$ becomes smaller than for the original gate sequence (thereby using possibly even a larger number of quantum gates). They considered as an example perturbations of the form $\delta H = V\delta$ with V being represented by a N -dimensional matrix randomly chosen from the Gaussian unitary ensemble (GUE). Thus, on average the matrix elements of V fulfill the condition $\langle V_{jk} V_{lm} \rangle = \delta_{jm} \delta_{kl} / N$. With this kind of imperfections on average the correlation function

becomes

$$\langle C(j, k) \rangle = \delta^2 \left(\left| \frac{1}{N} \text{tr}\{U_{j\dots 1} U_{1\dots k}^\dagger\} \right|^2 - \frac{1}{N^2} \right). \quad (33)$$

The $1/N^2$ -term comes from the fact that according to our assumption of traceless perturbing Hamiltonians also our matrices V have to be chosen traceless. (In the case of a non-traceless perturbations V this restriction can be achieved by the replacement $V \mapsto V - \mathcal{I} \text{tr} V / N$.) It should be mentioned that this latter $1/N^2$ -term was not taken into account in reference [18] so that these authors investigated the quantity $\delta^2 \left| \frac{1}{N} \text{tr}\{U_{j\dots 1} U_{1\dots k}^\dagger\} \right|^2$.

In order to demonstrate their idea, Prosen and Žnidarič considered the Quantum-Fourier-Transformation (QFT) as an example. Typically, this unitary transformation U is decomposed into $n_g = \lfloor n_q(n_q + 2)/2 \rfloor$ quantum gates which involve Hadamard operations and one-qubit phase gates (compare with the left-hand side of Fig. 2). Instead, Prosen and Žnidarič used a different decomposition involving $n'_g = \lfloor n_q(2n_q + 1)/2 \rfloor$ quantum gates. In Figure 3 the correlation matrix $\langle C(j, k) \rangle$ is depicted for both gate decompositions. Compared to the conventional gate decomposition (left) the off-diagonal elements of this correlation matrix are suppressed significantly by this new gate decomposition (middle). Diagonal values are always constant, i.e. $(\langle C(j, j) \rangle + 1/N^2)/\delta^2 = 1$.

Though of interest this proposal of Prosen and Žnidarič leaves important questions unanswered. How can such an improved gate sequence be found for an arbitrary quantum algorithm? How can this be achieved for repeated iterations of a unitary quantum map? Is it possible to suppress all off-diagonal elements of the correlation function perfectly? As explained in the next subsection all these questions can be addressed and solved in a rather straightforward way utilizing NRD decoupling [7].

3.4 Stabilization of quantum computations by NRD decoupling

In this section it is demonstrated that the recently proposed Pauli-random-error-correction (PAREC) method [7] can be understood as a stabilization of a quantum computation using NRD decoupling. This method allows to stabilize quantum algorithms against static imperfections by converting the typically quadratic time dependences of the resulting fidelity decays (29) into a linear ones. So far only numerical evidence has been presented for this remarkable property [7]. In this section a rigorous formula for the time dependence of the average entanglement fidelity of a PAREC-stabilized iterated quantum algorithm is presented. It exhibits explicitly the quantitative dependence of this fidelity decay on all relevant characteristic physical parameters.

In the PAREC method before each elementary quantum gate U_i , $i = 1, \dots, n_g$ of the τ th iteration ($\tau = 1, \dots, t$) of a unitary transformation U a unitary quantum gate $r_i^{(\tau)} r_{i-1}^{(\tau)\dagger}$ is applied. Thereby, the unitary gates $r_i^{(\tau)}$ (with $r_0^{(1)} = \mathcal{I}$) are drawn at random from a decoupling set \mathcal{G} . In this particular NRD method (compare with Sect. 2.3) \mathcal{G} can always chosen to be an annihilator, such as \mathcal{P} (compare with (15)). Simultaneously the changes on the quantum algorithm due to these random unitary gates have to be compensated by replacing each elementary quantum gate U_i of the τ th iteration of the original algorithm by $\tilde{U}_i^{(\tau)} = r_i^{(\tau)} U_i r_i^{(\tau)\dagger}$. Furthermore, after the last quantum gate $\tilde{U}_{n_g}^{(t)}$ a final unitary gate $r_{n_g}^{(t)\dagger}$ is applied. As a result each iteration of a unitary transformation U is replaced by $2n_g$ unitary quantum gates so that after t iterations one obtains the result

$$\begin{aligned} U^t &= U \dots U U \\ &= r_{n_g}^{(t)\dagger} (\tilde{U}_{n_g}^{(t)} \dots r_3^{(t)} r_2^{(t)\dagger} \tilde{U}_2^{(t)} r_2^{(t)} r_1^{(t)\dagger} \tilde{U}_1^{(t)} r_1^{(t)} r_{n_g}^{(t-1)\dagger}) \dots \\ &\dots \times (\tilde{U}_{n_g}^{(2)} \dots r_3^{(2)} r_2^{(2)\dagger} \tilde{U}_2^{(2)} r_2^{(2)} r_1^{(2)\dagger} \tilde{U}_1^{(2)} r_1^{(2)} r_{n_g}^{(1)\dagger}) \dots \\ &\dots \times (\tilde{U}_{n_g}^{(1)} \dots r_3^{(1)} r_2^{(1)\dagger} \tilde{U}_2^{(1)} r_2^{(1)} r_1^{(1)\dagger} \tilde{U}_1^{(1)} r_1^{(1)}) \\ &\quad \equiv (U_{2n_g}^{(t)} \dots U_2^{(t)} U_1^{(t)}) \dots \\ &\dots \times (U_{2n_g}^{(2)} \dots U_2^{(2)} U_1^{(2)}) (U_{2n_g}^{(1)} \dots U_2^{(1)} U_1^{(1)}) \quad (34) \end{aligned}$$

with $U_{2k}^{(t)} = \tilde{U}_k^{(t)}$, $U_{2k-1}^{(t)} = r_k^{(t)} r_{k-1}^{(t)\dagger}$, $k = 1, \dots, n_g$. A particular PAREC implementation of the quantum Fourier transform (QFT) is schematically represented in Figure 2

for the special case of $n_g = 4$ qubits. Definitely, this random application of Pauli operations together with the associated change of elementary quantum gates does not affect any quantum algorithm.

In order to discuss the stabilizing properties of this particular NRD methods let us consider the static imperfections of the previous section. Thus, it is assumed that each quantum gate U_i , $i = 1, \dots, n_g$ is performed instantaneously while between any two of these quantum gates there is a perturbing time evolution originating from the static imperfections which can be described by the unitary time evolution operator $\exp(-i\delta H)$ with $\delta H = H_0 \Delta t / \hbar$. As shown in Appendix A for sufficiently small times such a static imperfection results in an average decay of the entanglement fidelity of the form

$$\begin{aligned} \mathbf{E}F_e(t) &= 1 - 2tn_g \frac{1}{N} \text{tr} \{ (\delta H)^2 \} \\ &\quad - 2t \sum_{j=1}^{n_g} \frac{1}{N} \mathbf{E} \text{tr} \{ U_j^\dagger r_j^\dagger \delta H r_j U_j r_j^\dagger \delta H r_j \} + \mathcal{O}(\delta^3) \\ &\geq 1 - 4tn_g \frac{1}{N} \text{tr} \{ (\delta H)^2 \} + \mathcal{O}(\delta H^3). \quad (35) \end{aligned}$$

Thereby, the last inequality can be obtained by recalling that $\text{tr}\{A^\dagger B\}$ constitutes a Hermitian inner product for which the Cauchy-Schwarz inequality applies. Equation (35) explicitly exhibits the dependence of the entanglement fidelity decay on the number n_g of elementary quantum gates and the strictly linear dependence on the numbers of iterations of the unitary transformation U .

Several straightforward improvements of the basic relation (35) are possible. If the durations Δt_j of the static imperfections between adjacent elementary quantum gates are not equal but depend on these gates, for example, (35) is modified according to

$$\mathbf{E}F_e(t) \geq 1 - t \frac{1}{N} \text{tr}\{H_0^2\} \sum_{j=1}^{n_g} (\Delta t_j + \Delta t_{\text{bb}})^2 + \mathcal{O}(\delta^3). \quad (36)$$

Thereby, t_{bb} denotes the duration of the perturbation after the random pulses.

It is also possible to apply the random gates not before each elementary quantum gate but less often. One random quantum gate between each iteration of a quantum algorithm, for example, is already enough to get rid of the terms of (28) quadratic in t . In this case (35) is replaced by the inequality

$$\mathbf{E}F_e(t) \geq 1 - t(n_g + 1)^2 \frac{1}{N} \text{tr}\{(\delta H)^2\} \quad (37)$$

at the expense that the term linear in t has a coefficient quadratic in the number of elementary quantum gates per iteration n_g .

In order to determine the decay of the average entanglement fidelity of a quantum memory stabilized by NRD decoupling we use (35) and specialize to the case of one iteration $t = 1$ of a quantum algorithm consisting of $n_g = n$ identity gates with a time $\Delta t/2$ between subsequent quantum gates. This way the time between pulses

becomes equal to Δt . Denoting the total interaction time between the qubits of the quantum memory by $T = n_g \Delta t$ one obtains the result

$$\begin{aligned} F_e(T = n\Delta t) &\approx 1 - 4n_g \frac{1}{N} \text{tr}\{H_0^2\} (\Delta t/2)^2 \\ &= 1 - T \Delta t \frac{1}{N} \text{tr}\{H_0^2\}. \end{aligned} \quad (38)$$

3.5 Static imperfections modeled by the Gaussian unitary ensemble

In this section it is explicitly shown that the PAREC method is capable of canceling the off diagonal terms of the correlation function $\langle C(j, k) \rangle$ (33) perfectly. Let us consider the stabilization properties of the PAREC method with respect to static imperfections which can be characterized by traceless perturbing Hamiltonians of the form $\delta H = H_0 \Delta t / \hbar \equiv (V - \mathcal{I} \text{tr} V / N) / \delta$ with V chosen randomly from the Gaussian unitary ensemble (GUE). These perturbations describe physical situations in which in each individual realization of a quantum algorithm the inter-qubit Hamiltonian perturbing the dynamics of the qubits of the quantum information processor is time independent but random. To eliminate such GUE-governed static imperfections we have to choose an annihilator, such as \mathcal{P} , as a random decoupling set. As a result the fidelity averaged over all possible random gate reduces to the expression

$$\mathbf{E}\langle F_e \rangle = 1 - \sum_{j,k=1}^{n'_g} \mathbf{E}\langle C(j, k) \rangle + \mathcal{O}(\delta H^3). \quad (39)$$

According to equation (34) in the evaluation of expectation value of the correlation function we have to consider $n'_g = 2n_g$ quantum gates. In view of the statistical independence of subsequent Pauli operations almost all off-diagonal terms of the correlation function vanish, i.e.,

$$\frac{\mathbf{E}\langle C(j, k) \rangle}{\delta^2} = \begin{cases} 1 - \frac{1}{N^2} & \text{if } j = k, \\ \left| \frac{1}{N} \text{tr} U_j \right|^2 - \frac{1}{N^2} & \text{if } j \text{ even and } j = k + 1, \\ \left| \frac{1}{N} \text{tr} U_k \right|^2 - \frac{1}{N^2} & \text{if } k \text{ even and } k = j + 1, \\ 0 & \text{else.} \end{cases} \quad (40)$$

Thereby, it has been taken into account that for all unitary matrices U the relation

$$\mathbf{E}|\text{tr}\{U_r\}|^2 = \frac{1}{N^2} \sum_{j=1}^{N^2} |\text{tr}\{U_{r_j}\}|^2 = \frac{1}{N^2} \quad (41)$$

holds since the average is performed over all unitary random Pauli gates $r \in \mathcal{P}$ which are elements of an orthonormal unitary error basis. As a result the expectation value of the entanglement fidelity becomes

$$\begin{aligned} \mathbf{E}\langle F_e \rangle &= 1 - 2n_g \delta^2 (1 - N^{-2}) \\ &\quad - 2\delta^2 \sum_{j=1}^{n_g} \left(\left| \frac{1}{N} \text{tr} U_j \right|^2 - N^{-2} \right) + \mathcal{O}(\delta^3) \\ &\geq 1 - 4n_g \delta^2 (1 - N^{-2}) + \mathcal{O}(\delta^3). \end{aligned} \quad (42)$$

Alternatively this expression can also be derived by substituting the relevant perturbing Hamiltonian δH into (35) and setting $t = 1$ in (35). For the special case of a quantum Fourier transform (QFT) the resulting values of $\mathbf{E}\langle C(j, k) \rangle$ are shown on the right-hand side of Figure 3. In this figure they are also compared to the corresponding values resulting from the improved QFT proposed by Prosen.

4 Combining dynamical decoupling and detected-jump error correction

In this section a combined error correction scheme is introduced which allows a restricted form of dynamic decoupling within a detected-jump error correcting quantum code space. The error suppressing properties of this combined error correcting scheme are investigated in the presence of spontaneous decay processes and coherent but unknown Heisenberg-type inter-qubit couplings within a quantum information processor. Simple approximate expressions are derived for the expected average fidelity decay of instantaneous decoupling sequences, which are then confirmed by numerical simulations.

4.1 Spontaneous decay

4.1.1 Fidelity decay due to spontaneous decay

If the qubits of a quantum information processor couple to their environment, spontaneous state changes can occur by emitting energy in form of photons, for example. Such processes cause state changes from an excited state of a qubit, say $|1\rangle$, to an energetically lower lying state, say $|0\rangle$. Let us assume for our subsequent discussion that this state $|0\rangle$ is the qubit's stable ground state. The dynamics of spontaneous decay processes based on photon emission can be described by a master equation in Lindblad form [19]

$$\dot{\rho} = -\frac{i}{\hbar} [H_S(t), \rho] + \frac{1}{2} \sum_{i=0}^{n_q-1} ([L_i, \rho L_i^\dagger] + [L_i \rho, L_i^\dagger]). \quad (43)$$

Here, ρ describes the density operator of the quantum register involving n_q distinguishable qubits. Their unitary dynamics are described by the Hamiltonian $H_S(t)$. Typically, these dynamics originate from externally applied quantum gates. The non-unitary aspects of the time evolution of the quantum register are described by the Lindblad operators

$$L_k = \sqrt{\kappa_k} |0\rangle_i \langle 1| \otimes \mathcal{I}_{j \neq k}, \quad k = 1, \dots, n_q \quad (44)$$

which describe the influence of spontaneous emission processes on the qubits of the quantum register. In (43) it is assumed that the distinguishable qubits are separated by a distance much larger than the wavelength of the spontaneously emitted photons. As a result, to a good degree of approximation the qubits couple to statistically independent reservoirs [19]. If the decay rates of the qubits κ_k are

all equal, it is possible to construct quantum codes capable of correcting the spontaneous-emission induced errors.

However, before addressing such error correcting quantum codes let us look briefly at the expected fidelity decay of a quantum memory under the influence of such spontaneous decay processes. For this purpose let us consider the fidelity

$$F(t) = \langle \psi(0) | \rho(t) | \psi(0) \rangle, \quad (45)$$

with $\rho(t)$ obeying equation (43) with the initial condition $\rho(0) = |\psi(0)\rangle\langle\psi(0)|$. If a spontaneous decay event affects qubit i an arbitrary state of this qubit is mapped onto its ground state $|0\rangle_i$. As a consequence the resulting n_q -qubit state is expected to have almost no overlap with the n_q -qubit state before the decay process. Therefore, the fidelity is expected to become very small as soon as a decay process has affected any of the n_q -qubits. If there are n_1 -qubits in excited states initially, the probability that no decay event takes place in a time interval of duration t is given by

$$p(t) = \exp(-n_1 \kappa t) \quad (46)$$

provided the spontaneous decay rate κ is the same for all qubits. Thus assuming that the fidelity drops to zero as soon a spontaneous decay process has taken place the average expected fidelity at time t is approximately given by $F(t) \approx p(t)$ [see also (20)].

4.1.2 Detected-jump correcting codes

Spontaneous decay events as described by (43) can be corrected by detected-jump correcting quantum codes [3]. Thereby, all modifications of the ideal dynamics which do not arise from any photon decay events are corrected passively by an encoding of the logical information in an appropriate decoherence free subspace (DFS). This DFS is spanned by all quantum state involving a constant number of excited (physical) qubits. In order to maximize the dimension of this DFS one may choose quantum state with $n_q/2$ excited qubits. In order to be able to correct also any single error due to spontaneous decay of a known qubit by unitary recovery operations one has to construct code words by bitwise complementary pairing. In the case of four physical qubits, for example, such a one-error detected-jump correcting quantum code space is spanned by the three orthogonal logical states

$$|c_0\rangle = \frac{1}{\sqrt{2}}(|0011\rangle + e^{i\varphi}|1100\rangle), \quad (47a)$$

$$|c_1\rangle = \frac{1}{\sqrt{2}}(|0101\rangle + e^{i\varphi}|1010\rangle), \quad (47b)$$

$$|c_2\rangle = \frac{1}{\sqrt{2}}(|0110\rangle + e^{i\varphi}|1001\rangle). \quad (47c)$$

Thereby, the value of relative phase φ can be chosen arbitrarily. A detailed discussion of these error correcting quantum codes and their recovery operations can be found

in reference [4]. In particular, it has been shown that provided the error position and error time is known the recovery operation

$$R_i = X_i \prod_{j \neq i} \text{CNOT}_{i,j} H_i \quad (48)$$

restores any quantum state perfectly. The time t_{rec} needed for this recovery operation can be estimated by the time needed for the performance of $n_q - 1$ controlled NOT gates.

In order to simplify computation on the code space it is advantageous to use subspaces of one-error detected-jump correcting quantum codes which are equipped with a formal tensor product structure and have been introduced by [21]. The main idea is to map each logical qubit onto two physical qubits, i.e. $|0\rangle_L \rightarrow |01\rangle_P$ and $|1\rangle_L \rightarrow |10\rangle_P$, and again supplementing these code words with their bitwise complements. In order to be able to distinguish between logical two-qubit code words, such as $|00\rangle$ and $|11\rangle_L$, for example, one has to introduce two additional physical ancilla qubits. Thus, for two logical qubits, for example, the resulting four code words are given by

$$|00\rangle_L \rightarrow \frac{1}{\sqrt{2}}(|01\ 01\ 01\rangle + |10\ 10\ 10\rangle), \quad (49a)$$

$$|01\rangle_L \rightarrow \frac{1}{\sqrt{2}}(|01\ 10\ 01\rangle + |10\ 01\ 10\rangle), \quad (49b)$$

$$|10\rangle_L \rightarrow \frac{1}{\sqrt{2}}(|10\ 01\ 01\rangle + |01\ 10\ 10\rangle), \quad (49c)$$

$$|11\rangle_L \rightarrow \frac{1}{\sqrt{2}}(|10\ 10\ 01\rangle + |01\ 01\ 10\rangle). \quad (49d)$$

This scheme encodes n_L logical qubits in $n_P = 2n_L + 2$ physical qubits. As outlined in [20] and [21] it is possible to construct simple universal logical gates on these code spaces. With these quantum codes any single spontaneous decay process can be corrected perfectly provided the appropriate recovery operation is performed perfectly.

Let us look briefly at the expected average fidelity decay of a quantum memory which is protected by these jump codes and whose qubits decay spontaneously. The probability that no spontaneous decay takes place during a recovery process is given by

$$p'(t_{rec}) = \exp(-n_q/2 \kappa t_{rec}) \quad (50)$$

since on average at most $n_q/2$ qubits are excited during the recovery operation. Up to a time t one expects an average number $n_e(t) = \frac{n_q}{2} \kappa t$ of decay events. Thus, at time t the fidelity of the quantum memory is approximately given by [20]

$$F(t) = p'(t_{rec})^{n_e(t)} = \exp\left(-\left(\frac{n_q \kappa}{2}\right)^2 t_{rec} t\right). \quad (51)$$

Comparing (51) with the corresponding uncorrected fidelity decay of (46) (with $n_1 = n_q/2$) one notices a significant improvement provided the number of qubits n_q is too large, i.e. $\kappa n_q t_{rec}/2 \ll 1$. However, for large numbers of qubits, i.e. $\kappa n_q t_{rec}/2 > 1$, this method does not

work. This shortcoming can be remedied by encoding the physical qubits in blocks so that each block can correct one decay event at a time and by using block-entangling gates, such as the ones introduced in references [20, 22]. As a result error correction fails only if more than one spontaneous decay process occurs in the same block during recovery and the fidelity decay can be suppressed considerably in comparison with (51).

4.2 Embedding EMD decoupling inside a one-error detected-jump correcting quantum code space

Let us now investigate to which extent additional errors originating from uncontrolled inter-qubit couplings can be corrected by embedding a suitably chosen decoupling procedure into the code space of a one-error detected-jump correcting quantum code.

For this purpose let us consider a case in which in addition to spontaneous decay events also static energy detunings and nearest neighbor interactions affect the physical qubits of a quantum memory. Correspondingly, the error Hamiltonian describing these inter-qubit couplings is given by

$$H_S(t) = \sum_{i=0}^{n_q-1} \hbar \delta_i Z_i + \sum_{K=X,Y,Z} \sum_{j=0}^{n_q-2} \hbar J_{K,j} K_j K_{j+1} \equiv H_0, \quad (52)$$

with X , Y and Z denoting the Pauli spin operators. Thereby, the quantities δ_i denote detunings which may arise from an external magnetic field, for example, and the parameters $J_{K,j}$ characterize the strengths of nearest neighbor couplings. In (52) it is assumed that the qubits are arranged on a linear chain.

The detected-jump correcting quantum codes introduced above rely on a DFS involving a constant number of excited qubits. Therefore, one cannot use arbitrary decoupling schemes for suppressing the influence of unwanted inter-qubit couplings, since in general they may also change the number of excitations in the code words and as a result the code space would be left. Within the set of Pauli operations only the Z and swap-type operations leave these DFSs invariant. So, we can use a combination of Z -based *flips* and a random decoupling based on the symmetric group \mathcal{S}_{n_q} of permutations acting on n_q -qubits (*swaps*) for performing dynamical decoupling inside a one-error detected-jump correcting quantum code space. Thus, according to the notions of Section 2 this constitutes an EMD decoupling method, embedding PDD flip-decoupling inside NRD swap-decoupling. In particular, flip-decoupling applies the flip-operation

$$U_F = Z \otimes \mathcal{I} \otimes Z \otimes \dots \otimes \mathcal{I} \quad (53)$$

after time intervals of duration, say τ . This has the effect of canceling all 2-qubit couplings of XX - and YY -type and cross terms involving X and Y Pauli operations up to second order average Hamiltonian theory. But it leaves Z - and ZZ -type couplings invariant. Thus, neglecting higher

order terms caused by XX - and YY -type couplings the resulting intermediate average Hamiltonian H'_0 is given by

$$H'_0 = \sum_{i=0}^{n_q-1} \hbar \delta_i Z_i + \sum_{j=0}^{n_q-2} \hbar J_{z,j} Z_j Z_{j+1}. \quad (54)$$

It should be noted that this type of EMD decoupling method is applicable only if the number of physical qubits used in the code is a multiple of four with a corresponding odd number of logical qubits. Otherwise the flip operation (53) maps some codewords from symmetric ($\varphi = 0$) to antisymmetric ($\varphi = \pi$) superposition states which causes the recovery to fail. After a time $\Delta t = m\tau$, where m is an even integer, swap-decoupling permutes the logical qubits by executing up to $n_q - 1$ pairwise swap operations (transpositions). These swap operations are chosen at random in such a way that all permutations of the logical qubits are equally probable. Keeping track of the applied permutations, one knows which physical qubit one has to address in order to access the information that was originally stored in, say, the first qubit. As a result of this procedure decoupling results from the fact that the code words effectively see changing coupling constants between their qubits.

4.2.1 Expression for the expected fidelity of flipswap decoupling

To estimate the fidelity decay of a quantum memory perturbed by H_0 and protected by the flipswap decoupling discussed in Section 4.2, we calculate the evolution of a pure state, say $|\psi\rangle$, under the influence of the effective toggling-frame error Hamiltonian, i.e.,

$$U(t = N\Delta t) = \mathcal{T} \prod_{j=0}^N \exp(-iH_0^{(j)} \Delta t / \hbar) \quad (55)$$

with

$$H_0^{(j)} = P_j^\dagger H'_0 P_j \quad (56)$$

and P_j denoting the toggling-frame Hamiltonian and the permutations chosen randomly and independently for each time interval. Up to second order perturbation theory after time t the quantum state is given by

$$|\psi(t)\rangle = \left(\mathcal{I} - i \sum_{j=1}^N H_0^{(j)} \Delta t / \hbar - \sum_{i=2}^N \sum_{j=1}^{i-1} H_0^{(i)} H_0^{(j)} (\Delta t / \hbar)^2 - \frac{1}{2} \sum_{j=1}^N H_0^{(j)^2} (\Delta t / \hbar)^2 \right) |\psi(0)\rangle \quad (57)$$

Comparing this state with the ideal state $|\psi\rangle$ yields the fidelity

$$\begin{aligned}
F_C &= \left\langle |\langle \psi | \psi(t) \rangle|^2 \right\rangle_P \\
&\approx 1 - \sum_{i,j=1}^N \left\langle \langle \psi | (H_0^{(i)} - \langle \psi | H_0^{(i)} | \psi \rangle) \right. \\
&\quad \times (H_0^{(j)} - \langle \psi | H_0^{(j)} | \psi \rangle) | \psi \rangle \left. \right\rangle_P (\Delta t / \hbar)^2 \\
&= 1 - N(\Delta t / \hbar)^2 \left(\langle \psi | \langle H_0'^2 \rangle_P | \psi \rangle - \langle \langle \psi | H_0' | \psi \rangle^2 \rangle_P \right) \\
&\quad - (N^2 - N)(\Delta t / \hbar)^2 \\
&\quad \times \left(\langle \psi | \langle H_0' \rangle_P^2 | \psi \rangle - \langle \langle \psi | H_0' | \psi \rangle \rangle_P^2 \right) \quad (58)
\end{aligned}$$

with $\langle \dots \rangle_P$ denoting the ensemble average over all possible permutations,

$$\langle A \rangle_P = \frac{1}{n_q!} \sum_{P_i \in \mathcal{S}_{n_q}} P_i^\dagger A P_i. \quad (59)$$

In order to find an explicit expression for the expected fidelity we need to calculate the ensemble averages of H_0' , $H_0'^2$ and $\langle \psi | H_0' | \psi \rangle^2$.

Let us start with the calculation of $\langle H_0' \rangle_P$. Since the initial state $|\psi\rangle$ is an encoded quantum state we are only interested in the part of the Hamiltonian which has its support on the code space. Therefore, it is convenient to introduce the projection operator on this code space Π . By combinatorial arguments one can show that the average of the term involving the detunings δ_i is given by

$$\Pi \left\langle \sum_{i=0}^{n_q-1} \hbar \delta_i Z_i \right\rangle \Pi = 0. \quad (60)$$

This is due to the fact that each qubit is influenced by any detuning equally often and that inside the code space exactly half of the qubits are in excited states. The averaging of the terms involving ZZ-type interactions is slightly more complicated. However, on the code space one obtains the relation

$$\begin{aligned}
\Pi \left\langle \sum_{i=0}^{n_q-1} \hbar J_{z,i} Z_i Z_{i+1} \right\rangle \Pi &= -\frac{1}{n_q-1} \sum_{i=0}^{n_q-1} \hbar J_{z,i} \Pi \\
&=: c_1 \Pi \quad (61)
\end{aligned}$$

with the real number c_1 depending on the strengths of the inter-qubit couplings $J_{z,i}$. Similarly, one can calculate $\langle H_0'^2 \rangle_P$. Cross terms of Z- and ZZ-type vanish after ensemble averaging. Remaining terms are proportional to \mathcal{I} , ZZ or ZZZZ. Averaging these latter terms over all per-

mutations results in

$$\begin{aligned}
\Pi \langle H_0'^2 / \hbar^2 \rangle_P \Pi &= \left[\sum_{i=0}^{n_q-1} \delta_i^2 - \frac{2}{n_q-1} \sum_{i<j} \delta_i \delta_j \right. \\
&\quad + \sum_{j=0}^{n_q-2} J_{z,j}^2 - \frac{2}{n_q-1} \sum_{i=0}^{n_q-3} J_{z,i} J_{z,i+1} \\
&\quad \left. + 2(p'_+ - p'_-) \sum_{j=2}^{n_q-2} J_{z,i} J_{z,j} \right] \Pi \\
&=: c_2 \Pi / \hbar^2, \quad (62)
\end{aligned}$$

with p'_\pm denoting the probability of finding four bits of a word with $n_q/2$ excited qubits arranged in such a way that applying the four-qubit operator ZZZZ to them yields the eigenvalue ± 1 . Furthermore, one finds the relation

$$p'_+ - p'_- = \frac{3}{3 - 4n_q + n_q^2}. \quad (63)$$

The last term one has to calculate is given by

$$\langle \langle \psi | H_0' | \psi \rangle^2 \rangle_P =: c_3, \quad (64)$$

and depends on the initial state $|\psi\rangle$. This initial state can always be expressed as a superposition of the symmetric ($\varphi = 0$) basis states, i.e. $|\psi\rangle = \sum_k a_k |\psi_k\rangle$ with $\sum_k |a_k|^2 = 1$. Therefore, detunings do not matter, since the application of any Z_i operator to any symmetric basis state changes it into its antisymmetric pendant and vice versa. It is not difficult to prove the following upper and lower bounds for the positive constant c_3

$$c_1^2 \leq c_3 \leq \left(c_2 - \sum_{i=0}^{n_q-1} \hbar^2 \delta_i^2 + \frac{2\hbar^2}{n_q-1} \sum_{i<j} \delta_i \delta_j \right). \quad (65)$$

In general, the value of the quantity c_3 depends on the quantum state. The upper bound corresponds to the case $a_i = \delta_{i0}$ and the lower bound to the case $a_i = \text{const}$.

Inserting these results into the fidelity (58), the quadratic-in-time term vanishes since $\Pi \langle H_0' \rangle_P \Pi \propto \Pi$. With $t_0 = 0$ the fidelity due to coherent errors becomes independent of the initial state $|\psi\rangle$ and is given by

$$F_C \approx 1 - t \Delta t (c_2 - c_1^2) / \hbar^2 \quad (66)$$

with Δt denoting the time between subsequent swap operations. Thus, a linear-in-time fidelity decay is obtained due to the fact that the EMD decoupling suppresses the quadratic-in-time decay resulting from inter-qubit couplings. This is a main results of this section. This calculated linear can be used as the leading order of an exponential approximation yielding the fidelity decay

$$F_C \approx \exp(-t \Delta t (c_2 - c_1^2) / \hbar^2). \quad (67)$$

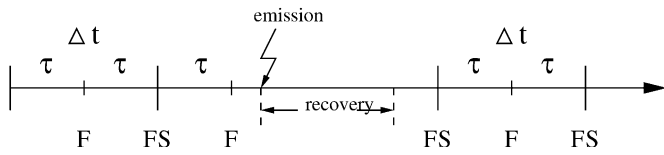


Fig. 4. A typical sequence of instantaneously applied flip-type (F) and swap-type (S) decoupling operations and of a recovery operation of duration t_{rec} : during recovery no decoupling operations are executed. Here the time delay between swap operations Δt and the time delay between subsequent flip operations τ are related by $\Delta t = 2\tau$.

4.2.2 Implementations and numerical simulations

In a practical implementation of the combined scheme discussed above one corrects spontaneous decay events with priority by taking into account that recovery operations must not be interrupted by decoupling operations. This compatibility requirement guarantees that no additional uncorrectable errors occur during the recovery steps. A corresponding typical correction sequence is depicted schematically in Figure 4. This compatibility requirement may lead to varying time intervals between individual decoupling operations. However, for the decoupling scheme discussed here this does not present any serious problems. Assuming that a successful recovery operation recovers a faulty state perfectly while a failed recovery approximately results in a vanishing fidelity, the fidelity decay of such a combined error correcting scheme is given by products of the fidelities of equations (51) and (67).

In the following we discuss the fidelity decay in the idealized case of instantaneous decoupling operations. However, the recovery operation is assumed to require always a finite total time which grows linearly with the number of qubits involved (compare with (48)),

$$t_{rec} = \left(\frac{3}{2}(n_q - 1) + 2 \right) t_0. \quad (68)$$

Therefore, secondary spontaneous decays during a recovery cause errors. Composite gates, such as CNOT gates, are assumed to take $3/2$ times as long as the basic gate time t_0 .

4.2.3 Instantaneously applied decoupling operations

Let us assume that the deterministic flip operations and stochastic swap operations are performed instantaneously after time intervals of duration τ and $\Delta t = m\tau$ with an even integer m (compare with Fig. 4). Whenever a spontaneous decay event occurs between two flip operations the recovery operation is applied and the decoupling sequence is halted for a time interval of duration t_{rec} . Furthermore, we are primarily interested in cases of frequent decouplings, i.e. $t_{rec} \gg \tau$, with spontaneous decay representing a weak perturbation, i.e. $\kappa\tau \ll 1$. Thus, according to equations (51) and (67) after time $t = N\Delta t$ the expected fidelity F_{ID} of a quantum memory whose dynamics

are governed by the master equation (43) with Hamiltonian (52) is approximately given by

$$F_{ID} = \exp\left(- (c_2 - c_3)(t\Delta t/\hbar^2)(1 + \kappa t_{rec}n_q/2)\right) \times \exp\left(- \left(\frac{n_q\kappa}{2}\right)^2 t_{rec}t\right) \quad (69)$$

with $n_{ph} = (n_q/2)\kappa t$ denoting the mean number of spontaneous decay events taking place during the time interval $t = N\Delta t$. Thus, in order to maximize this fidelity it is optimal to minimize the decoupling time interval Δt .

4.3 Numerical results

Let us assume that the coupling constants δ_j and $J_{z,j}$ of the Hamiltonian (52) are time independent but unknown and that they are distributed randomly and uniformly in the interval $[-\sqrt{3}\epsilon, \sqrt{3}\epsilon]$. In the following we discuss the time evolution of the fidelity of a quantum memory with three logical qubits in a coherent state perturbed by spontaneous decay processes and by inter-qubit couplings (compare with Eqs. (43) and (52)). The numerical simulations were performed with the help of the quantum trajectory method [23]. Random elements which had to be averaged over several trajectories were the realizations of random swap operations on the one hand and times and positions of spontaneous decay processes on the other hand.

In the case of instantaneous decoupling operations it is best to apply them as often as possible as assumed in (69), for example. Figure 5 shows a 3-qubit and an 8-qubit encoded quantum memory. The curves drawn correspond to the cases of no decoupling and error correction at all (red \diamond), of decoupling only (blue \circ), of error correction by a jump code only (light blue $+$), and of the combined scheme discussed here (pink \times). The characteristic quadratic-in-time fidelity decay due to coherent errors is apparent from the curves without decoupling (blue \circ). This decay is superimposed by a (fast) linear-in-time decay due to (un)corrected spontaneous decay. The more frequently one applies decoupling operations, the closer one gets to the spontaneous-decay-induced limit described by (51).

5 Summary

Two applications for random decoupling have been presented.

In Section 3 it was shown that random decoupling can be used to stabilize quantum algorithms against static imperfections in an efficient way. In particular, a simple expression was derived for the average fidelity decay of a quantum memory emerged which complements already known rigorous lower bounds for the worst case behaviour.

In Section 4 it has been demonstrated that errors originating from uncontrolled couplings to an environment and from couplings among qubits of a quantum information processor can be corrected efficiently by combining

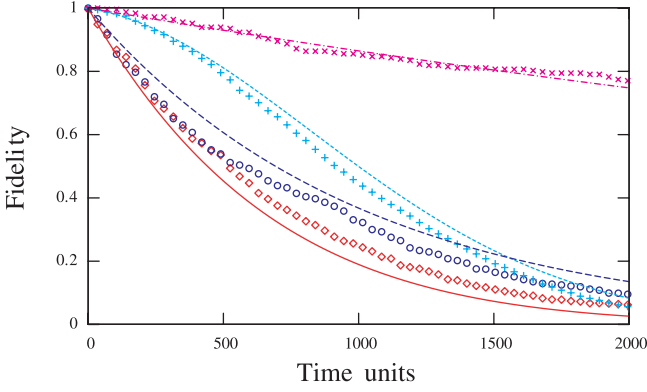


Fig. 5. (Color online) Time evolution of the average fidelity whose dynamics are governed by equation (43): 3 physical qubits without any error correction or decoupling (red \diamond), 3 physical qubits with instantaneous dynamical decoupling only with $\Delta t = 4t_0$ (blue \circ), 8 physical qubits encoding 3 logical qubits with combined error correction and instantaneous decoupling with $\Delta t = 4t_0$ (pink \times), 8 physical qubits encoding 3 logical qubits (light blue $+$) without decoupling. (The time is plotted in units of the elementary gate time t_0 .) The full lines represent the corresponding approximate analytical expressions given in the text. The parameters are $\kappa t_0 = 10^{-3}$, $\epsilon t_0 = 10^{-4}$. Statistical fluctuations originate from the sampling of the permutations. In the curve for $n_q = 8$, for example, 500 random permutations are chosen per quantum trajectory over a total of 100 trajectories which is only slightly more than the size of the permutation group ($8! = 40320$).

redundancy-based quantum error correction with dynamical decoupling methods. In the particular example presented an embedded dynamical decoupling scheme was embedded into a one-error correcting detected-jump correcting quantum code. This way both spontaneous decay processes and uncontrolled inter-qubit couplings could be suppressed significantly. An important aspect which has to be taken into account in the development of such combined error suppression methods is compatibility. It has to be ensured that the dynamical decoupling operations used do not leave the code space of the redundancy-based quantum error correcting quantum code. Typically this compatibility requirement constrains the structure of the admissible dynamical decoupling operations.

This work is supported by the DAAD. I.J. acknowledges also financial support by project MSM 6840770039. Stimulating discussions with Dima L. Shepelyansky are acknowledged.

Appendix A

In this appendix the perturbative short-time approximation of the fidelity amplitude used in (28) is derived. Let us consider a quantum algorithm iterating an ideal unitary transformation $U = U_{n_g} \cdots U_3 U_2 U_1$ t times. If this ideal time evolution is perturbed by static imperfections originating from Hamiltonian inter-qubit couplings the j th

quantum gate of the τ th iteration of U is replaced by the perturbed unitary quantum gate

$$U_j \mapsto \exp(-i\delta H_{jl}^\tau) U_j \exp(-i\delta H_{jr}^\tau). \quad (70)$$

In equation (28), for example, the special case $\delta H = H_0 \Delta t$ and $\delta H_{jr}^\tau = 0$ is considered. The index τ in (70) takes into account that perturbations may be different in successive iterations of the unitary transformation U . In a second order expansion with respect to δH_{jl}^τ and δH_{jr}^τ after t iterations the fidelity amplitude A (25) of the iterated perturbed quantum algorithm is given by

$$\begin{aligned} A(t) = & 1 - \sum_{p=l,r} \sum_{\tau=1}^t \sum_{j=1}^{n_g} \frac{1}{N} \left(i \operatorname{tr}\{\delta H_{jp}^\tau\} - \frac{1}{2} \operatorname{tr}\{(\delta H_{jp}^\tau)^2\} \right) \\ & - \sum_{\tau=1}^t \sum_{j=2}^{n_g} \sum_{k=1}^{j-1} \frac{1}{N} \left[\operatorname{tr}\{\delta \tilde{H}_{jl}^\tau(j) \delta \tilde{H}_{kl}^\tau(k)\} \right. \\ & + \operatorname{tr}\{\delta \tilde{H}_{jl}^\tau(j) \delta \tilde{H}_{kr}^\tau(k-1)\} \\ & + \operatorname{tr}\{\delta \tilde{H}_{jr}^\tau(j-1) \delta \tilde{H}_{kl}^\tau(k)\} \\ & \left. + \operatorname{tr}\{\delta \tilde{H}_{jr}^\tau(j-1) \delta \tilde{H}_{kr}^\tau(k-1)\} \right] \\ & - \sum_{\tau=1}^t \sum_{j=1}^{n_g} \frac{1}{N} \operatorname{tr}\{U_j^\dagger \delta H_{jl}^\tau U_j \delta H_{jr}^\tau\} \\ & - \sum_{\tau_1=2}^t \sum_{\tau_2=1}^{\tau_1-1} \sum_{j,k=1}^{n_g} \frac{1}{N} \\ & \times \left[\operatorname{tr}\{U^{\tau_2-\tau_1} \delta \tilde{H}_{jl}^{\tau_1}(j) U^{\tau_1-\tau_2} \delta \tilde{H}_{kl}^{\tau_2}(k)\} \right. \\ & + \operatorname{tr}\{U^{\tau_2-\tau_1} \delta \tilde{H}_{jl}^{\tau_1}(j) U^{\tau_1-\tau_2} \delta \tilde{H}_{kr}^{\tau_2}(k-1)\} \\ & + \operatorname{tr}\{U^{\tau_2-\tau_1} \delta \tilde{H}_{jr}^{\tau_1}(j-1) U^{\tau_1-\tau_2} \delta \tilde{H}_{kl}^{\tau_2}(k)\} \\ & \left. + \operatorname{tr}\{U^{\tau_2-\tau_1} \delta \tilde{H}_{jr}^{\tau_1}(j-1) U^{\tau_1-\tau_2} \delta \tilde{H}_{kr}^{\tau_2}(k-1)\} \right] \\ & + \mathcal{O}(\delta H^3) \end{aligned} \quad (71)$$

with

$$\begin{aligned} \delta \tilde{H}_{jp}^\tau(i) &= U_1^\dagger U_2^\dagger \cdots U_i^\dagger \delta H_{jp}^\tau U_i \cdots U_2 U_1 \\ &= U_{1\dots i}^\dagger \delta H_{jp}^\tau U_{i\dots 1}. \end{aligned} \quad (72)$$

The term linear in the perturbing Hamiltonian δH vanishes if all Hamiltonians involved are traceless. Note that all the terms of (71) involving $\operatorname{tr}\{\cdot\}$ terms are real valued so that up to second order the fidelity $F_e(t) = |A(t)|^2$ is simply obtained by multiplying all these terms of $A(t)$ with a factor of magnitude two. In the special case $\delta H_{jl}^\tau = \delta H = H_0 \Delta t$, $\delta H_{jr}^\tau = 0$ (71) gives rise to equation (28).

Setting $\delta H_{il}^\tau = \delta H_{ir}^\tau = r_i^{(\tau)\dagger} \delta H r_i^{(\tau)}$ equation (71) yields the time evolution of (34). Performing an average \mathbf{E} over all random unitary operations $\{r_i^{(\tau)}\}$ from the decoupling

set \mathcal{G} one obtains the expectation value of the amplitude

$$\begin{aligned} \mathbf{E}A(t) &= 1 - \sum_{\tau=1}^t \sum_{j=1}^{n_g} \frac{1}{N} \operatorname{tr}\{(r_j^{(\tau)\dagger} \delta H r_j^{(\tau)})^2\} \\ &- \sum_{\tau=1}^t \sum_{j=1}^{n_g} \frac{1}{N} \mathbf{E} \operatorname{tr}\{U_j^\dagger r_j^{(\tau)\dagger} \delta H r_j^{(\tau)} U_j r_j^{(\tau)\dagger} \delta H r_j^{(\tau)}\} + \mathcal{O}(\delta^3). \end{aligned} \quad (73)$$

References

1. L. Viola, E. Knill, S. Lloyd, Phys. Rev. Lett. **82**, 2417 (1999)
2. M.A. Nielsen, I.L. Chuang, *Quantum Computation and Quantum Information* (Cambridge University Press, Cambridge, UK, 2000)
3. G. Alber, T. Beth, C. Charnes, A. Delgado, M. Grassl, M. Mussinger, Phys. Rev. Lett. **86**, 4402 (2001)
4. G. Alber, T. Beth, C. Charnes, A. Delgado, M. Grassl, M. Mussinger, Phys. Rev. A **68**, 012316 (2003)
5. O. Kern, G. Alber, Phys. Rev. Lett. **95**, 250501 (2005)
6. L. Viola, E. Knill, Phys. Rev. Lett. **94**, 060502 (2005)
7. O. Kern, G. Alber, D.L. Shepelyansky, Eur. Phys. J. D **32**, 153 (2005)
8. R.R. Ernst, G. Bodenhausen, A. Wokaun, *Principles of Nuclear Magnetic Resonance in One and Two Dimensions of series International Series of Monographs on Chemistry* (Oxford Science Publications, 1987), Vol. 14
9. M. Stollsteimer, G. Mahler, Phys. Rev. A **64**, 052301 (2001)
10. L.F. Santos, L. Viola, Phys. Rev. Lett. **97**, 150501 (2006)
11. P. Wocjan, M. Rotteler, D. Janzing, T. Beth, Quant. Inf. Comp. **2**, 133 (2002)
12. E. Knill, *Non-binary unitary error bases and quantum codes*, Technical report LAUR-96-2717, Los Alamos National Laboratory, arXiv:quant-ph/9608048 (1996)
13. T. Prosen, Phys. Rev. E **65**, 036208 (2002)
14. M.A. Nielsen, Phys. Lett. A **303**, 249 (2002)
15. D. Poulin, R. Blume-Kohout, R. Laflamme, H. Ollivier, Phys. Rev. Lett. **92**, 177906 (2004)
16. L.K. Grover, Phys. Rev. Lett. **79**, 325 (1997)
17. K.M. Frahm, R. Fleckinger, D.L. Shepelyansky, Eur. Phys. J. D **29**, 139 (2004)
18. T. Prosen, M. Žnidarič, J. Phys. A: Math. Gen. **34**, L681 (2001)
19. H. Carmichael, *Statistical Methods in Quantum Optics* (Springer, 2003)
20. O. Kern, G. Alber, Eur. Phys. J. D **36**, 241 (2005)
21. K. Khodjasteh, D.A. Lidar, Phys. Rev. Lett. **89**, 197904 (2002)
22. G. Alber, M. Mussinger, A. Delgado, *Universal sets of quantum gates for detected jump-error correcting quantum codes*, e-print arXiv:quant-ph/0208177 (2002)
23. R. Dum, A.S. Parkins, P. Zoller, Phys. Rev. A **46**, 4382 (1992)